Published online October 4, 2004

Nucleic Acids Research, 2004, Vol. 32, No. 17 ***5163–5173***
doi:10.1093/nar/gkh847

Position- and orientation-specific enhancement of topoisomerase I cleavage complexes by triplex DNA structures

Smitha Antony, Paola B. Arimondo[1], Jian-Sheng Sun[1] and Yves Pommier*

Laboratory of Molecular Pharmacology, Center for Cancer Research, National Cancer Institute, National Institutes of Health, Bethesda, MD 20892-4255, USA and [1]USM 0503 Muséum National d'Histoire Naturelle, UMR 5153 CNRS-MNHN, INSERM U565, 43 rue Cuvier, BP26, 75231 Paris cedex 05, France

Received May 8, 2004; Revised July 27, 2004; Accepted September 7, 2004

ABSTRACT

Topoisomerase I (Top1) activities are sensitive to various endogenous base modifications, and anticancer drugs including the natural alkaloid camptothecin. Here, we show that triple helix-forming oligonucleotides (TFOs) can enhance Top1-mediated DNA cleavage by affecting either or both the nicking and the closing activities of Top1 depending on the position and the orientation of the triplex DNA structure relative to the Top1 site. TFO binding 1 bp downstream from the Top1 site enhances cleavage by inhibiting religation and to a lesser extent DNA nicking. In contrast, TFO binding 4 bp downstream from the Top1 site enhances DNA nicking especially when the 3′ end of the TFO is proximal to the Top1 site. However, when the orientation of the triplex is inverted, with its 5′ terminus 4 bp downstream from the Top1 site, religation is also inhibited. These position- and orientation-dependent effects of triplex structures on the Top1-mediated DNA cleavage and religation are discussed in the context of molecular modeling and effects of TFO on DNA twist and mobility at the duplex/triplex junction.

INTRODUCTION

DNA topoisomerases play a vital role during cellular metabolic processes such as replication, transcription, recombination and repair when DNA relaxation is of essence (1–4). DNA topoisomerases have been referred to as guardians of the genome (5) or genome gate keepers (6) with the potential of harming the genome when their activity is perturbed (4,6–9) (see reviews at http://discover.nci.nih.gov/pommier/pommier.htm). By nicking one DNA strand, allowing controlled rotation and religating (closing) the break (see scheme in Materials and Methods), topoisomerase I (Top1) relieves the torsional strain generated by DNA tracking during transcription and replication. DNA, however, being a dynamic molecule can exist in different forms (10). Depending on the nucleotide sequence and its environment, DNA can form multistranded helices through either the folding of a single strand or the association of two, three or four strands (11). In particular, the binding of a third strand in the major groove of an oligopyrimidine•oligopurine DNA stretch forms a local triple-helical structure called triple helix or triplex (12). Using bioinformatics tools, it has been shown that sequences able to form triplexes are widespread in the genome (13). More importantly, triple helix-forming oligonucleotide (TFO) target sequences have been found in regulatory regions, especially in promoter zones and recombination hot spots of eukaryotic DNA (14). It is likely that such unusual structures may play an important role in controlling the functions of the genome.

Several studies have taken advantage of the specificity of the recognition process between the TFO and duplex DNA to develop sequence-specific gene targeting reagents in cells. Depending on the desired effect, triplexes have been used to knock down/out specific genes, direct nuclease cutting, construct artificial restriction enzymes, induce recombination, chromatin remodeling and transposon insertion or induce specific mutations in the genome (15). TFOs covalently linked to anticancer drugs like camptothecin (CPT) and indolocarbazole derivatives that target Top1 have helped in mediating selectivity of the drug to a target sequence and increasing the drug efficacy at these sites (16). This enhanced effect of a TFO-drug conjugate versus the unconjugated drug was found to be dependent on the 3′ and 5′ position of the TFO–drug conjugate relative to the DNA cleavage site (17). An unexpected result was the enhanced Top1-mediated DNA cleavage by the triple-helical structure alone (17).

The present study was undertaken to understand how multistranded DNA structures like triplexes influence the activity of Top1. To characterize the site-specific effects of triplexes on Top1 cleavage activity, we introduced the triplex site starting with one or four bases 3′ from a well-characterized Top1 cleavage site (18–23). In a second set of experiments, we altered the sequence of the DNA between the Top1 cleavage site and the triplex site to study the role of the DNA sequence in the effect of triplexes on Top1 cleavage activity. Finally, we reversed the orientation of the triplex to see whether it differentially affected the Top1 cleavage (17).

*To whom correspondence should be addressed at Laboratory of Molecular Pharmacology, Center for Cancer Research, National Cancer Institute, 37 Convent Drive, Building 37, Room 5068, National Institutes of Health, Bethesda, MD 20892-4255, USA. Tel: +1 301 496 5944; Fax: +1 301 402 0752; Email: pommier@nih.gov

MATERIALS AND METHODS

Drugs, enzymes and chemicals

CPT was obtained from the Drug Synthesis and Chemistry Branch, National Cancer Institute (Bethesda, MD). Drug stock solutions were made in dimethyl sulfoxide (DMSO) at 10 mM. Aliquots were stored at −20°C and further dilutions were made in DMSO immediately before use. The final concentration of DMSO in the reaction did not exceed 10% (v/v).

Recombinant human Top1 was purified from TN5 insect cells (HighFive, Invitrogen Corp., San Diego, CA) using a Baculovirus construct for the N-terminus truncated human Top1 cDNA as described previously (21). Terminal deoxynucleotidyl transferase, dNTP [where N is A (adenosine), C (cytosine), G (guanosine) or T (thymine)], agarose and polyacrylamide/bis were purchased from GIBCO BRL (Gaithersburg, MD) or New England Biolabs (Beverly, MA). Oligo quick spin columns were purchased from Roche Diagnostics Corporation (Indianapolis, IN). [α^{32}-P]-cordycepin 5′-triphosphate was purchased from DuPont-New England Nuclear (Boston, MA). Oligonucleotides were synthesized by MWG-Biotech (High Point, NC).

Top1 reactions

Single-stranded oligonucleotides were 3′ labeled with [α^{32}-P]-cordycepin and terminal deoxynucleotidyl transferase as described in (19–21). Labeling mixtures were subsequently centrifuged through mini quick spin Oligo columns (Roche Diagnostics Corporation) to remove the unincorporated [α^{32}-P]-cordycepin. Annealing to the unlabeled complementary strand was performed in 1× annealing buffer (10 mM Tris–HCl, pH 7.8, 100 mM NaCl, 1 mM EDTA) by heating the reaction mixtures to 95°C for 5 min, followed by slow cooling to room temperature.

Triplex formation

TFOs were purchased from Eurogentec (Belgium) on the 0.2 μmol scale and purified using Micro Bio-Spin® 6 Chromatography columns (Bio-Rad, Hercules, CA). Concentrations were determined spectrophotometrically at 25°C using molar extinction coefficients at 260 nm calculated from a nearest-neighbor model (24). The TFO is complementary to the oligopurine strand of the duplex and parallel to it. The orientation of the triplex is defined as the orientation of the oligopurine strand of the duplex. Triplex formation was carried out as described in (17). Briefly, the radiolabeled target duplex (50 nM) was incubated for 2 h at 30°C in 50 mM Tris–HCl, pH 7.5, 60 mM KCl, 10 mM $MgCl_2$, 0.5 mM dithiothreitol, 0.1 mM EDTA and 30 μg/ml of BSA, in the presence of the TFO (1 μM) to form the triplex (total reaction volume, 20 μl).

For Top1 cleavage assays, labeled duplex or triplex DNA (~50 fmol/reaction) was incubated with 5 ng of recombinant Top1 with or without drug at either 25 or 0°C in 10 μl reaction buffer (10 mM Tris–HCl, pH 7.5, 50 mM KCl, 5 mM $MgCl_2$, 0.1 mM EDTA, 15 μg/ml BSA, final concentrations). Reactions were stopped by adding SDS (0.5% final concentration). For reversal experiments, the SDS stop was preceded by the addition of NaCl to a final concentration of 0.35 M followed by incubation for varying time points (min) at either 0, 25 or 37°C.

To the reaction mixtures, 3.3 vol of Maxam Gilbert loading buffer (80% formamide, 10 mM NaOH, 1 mM NaEDTA, 0.1% xylene cyanol and 0.1% bromophenol blue, pH 8.0) was added. Aliquots were separated in 20% denaturing polyacrylamide gels (7 M urea) in 1× TBE (89 mM Tris-borate, 2 mM EDTA, pH 8.0) for 2 h at 40 V/cm at 50°C.

Imaging was performed using a Phosphorimager (Molecular Dynamics, Sunnyvale, CA). Quantification of the labeled DNA bands was performed using the software ImageQuant (that calculates the intensity of the band/product within a given area). Then the percent cleavage of product was calculated relative to the total product + the substrate.

Calculation of the cleavage (k_1) and religation (k_2) rate constants for triplex and CPT-induced Top1-mediated DNA cleavage

The normal catalytic cycle of Top1 consists of two transesterification reactions. The first transesterification cleaves the DNA backbone by nucleophilic attack of the enzyme active tyrosine (Tyr-723 in humans) to form a covalent enzyme–DNA complex. The rate of this forward (nicking) reaction is denoted as k_1. Top1 catalyzes a second transesterification that religates the ends of the broken DNA. The rate of this reverse reaction (closing) is denoted as k_2. Under normal conditions, the Top1-mediated cleavage is transient ($k_2 \gg k_1$). CPT traps the Top1-cleavage complex by inhibiting religation reversibility (i.e. by decreasing k_2). This can be represented schematically as follows:

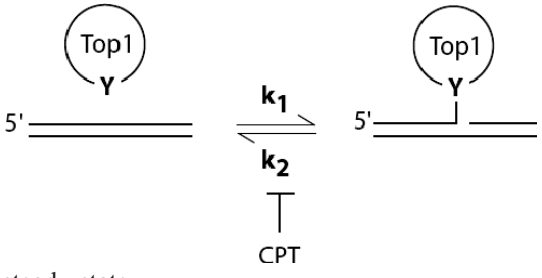

At steady state,

$$k_1 \times (1 - r) = k_2 \times r$$

In the presence of salt (NaCl) assuming that $k_1 = 0$, the time taken for half of the cleaved product to reverse ($T_{1/2}$) was calculated from the semilog plot of the percentage of cleavage product remaining after the salt reversal experiments (see Figures 3B, 3C, 4D, 4E, 5E and 6E).

The religation rate k_2 was calculated as

$$k_2 = \text{Ln } 2/T_{1/2}$$

The cleavage rate k_1 was calculated as

$$k_1 = k_2 \times r/(1 - r)$$

where r is the fraction of cleavage product at the plateau (see Figures 2C, 4C, 5D and 6D). Derivations of these equations are described in detail in (25).

Molecular modeling

Molecular modeling was performed by conformational energy minimization with Jumna program package (version 10.3)

(26). Neither water nor positively charged counter ions were explicitly included in the energy minimization. However, their effects were simulated by a sigmoidal, distance-dependent, dielectric function (27), and by assignment of a half-negative charge for each phosphate group. Computations were carried out on a PC under Linux.

The structures containing duplex–triplex junction were built and energy minimized as described previously (28). The B80 coordinates of DNA double helix and the coordinates of DNA triple helices, which were derived from the previously published B-like triple helix (29), were used for the construction of duplex and triplex, respectively.

Adiabatic mapping was carried out in order to assess the local twist flexibility at the scission site (two or five step away from the junction for 27 or 30mer, respectively). In short, the calculations were performed in a stepwise way starting from the energy minimum with 1° increment.

RESULTS

Formation of a triplex 1 bp 3′ from the Top1–DNA cleavage site enhances cleavage by inhibiting the religation reaction

Figure 2B shows that the presence of the triplex one base from the Top1 cleavage site (sequence shown in Figures 1 and 2A) enhanced the Top1-mediated DNA cleavage (+TFO) as compared with Top1 alone (160 Top1). This enhancement increased with the time (+TFO, 1–160 min) of Top1 reaction

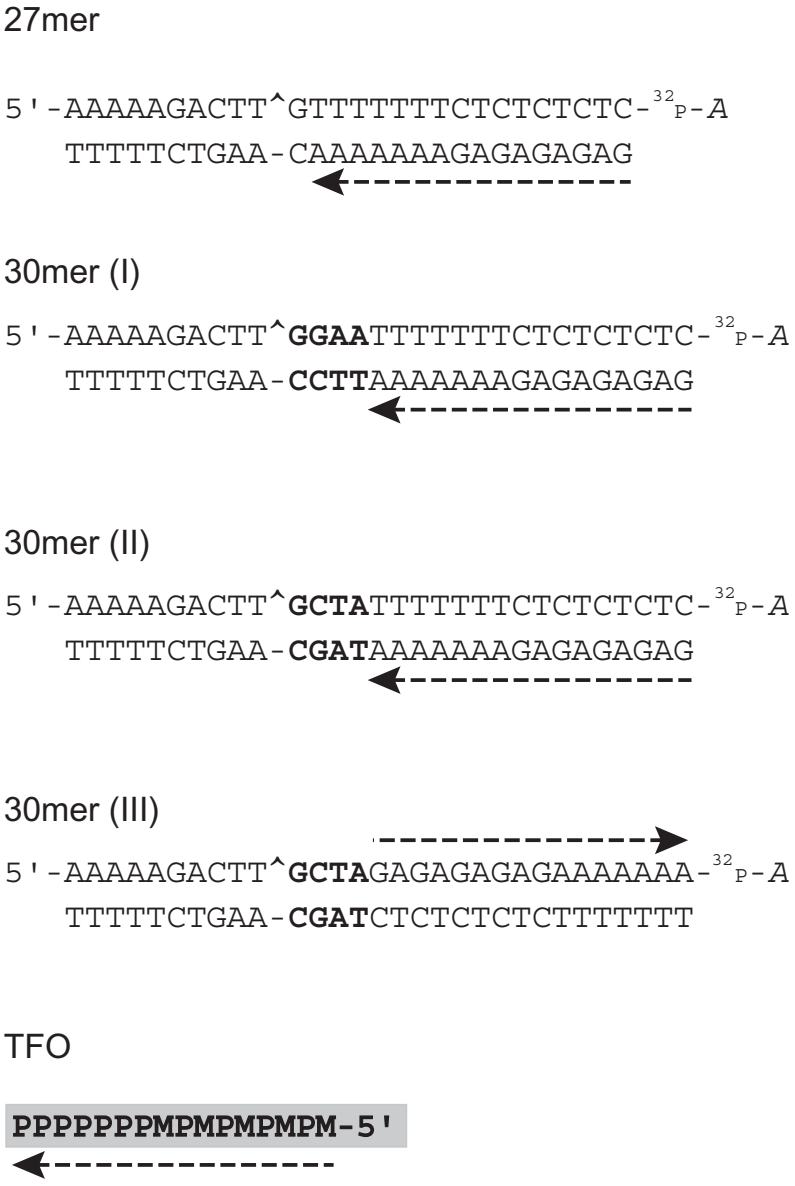

Figure 1. Sequences of the oligonucleotides used for this study. Sequences of the target 27, 30mer (I), (II) and (III) duplex oligonucleotides and the TFO showing the 3′ radiolabel (cordycepin indicated by ^{32}P-*A*) on the scissile strand of the duplexes. The TFO binds in the major groove in a parallel orientation to the oligopurine strand of the duplex and is indicated by a dashed arrow. The Top1-mediated DNA cleavage site is indicated by a caret (^), and the nucleotides between the site of cleavage and formation of the triplex are highlighted in bold. **M**, 5-methyl-2′-deoxycytidine; **P**, 5-propynyl-2′-deoxyuridine.

at a slower rate in the presence of the triplex than in the presence of +CPT (see Figure 2B and C).

To determine the effect of TFO on the religation reaction, the stability of the Top1-mediated DNA cleavage complex was tested by salt reversal experiments and compared with CPT, a known inhibitor of the Top1-mediated DNA religation (as 21,30,31) (http://discover.nci.nih.gov/pommier/pommier.htm). Kinetic analyses of the rate of reversal of the complexes at different temperatures (0, 25 and 37°C; Figure 3 and Table 1) showed the religation rate (k_2) to be slower for TFO than for CPT. Lowering the temperature at which religation of the complexes was carried out slowed down the religation process (Figure 3B and C) (31), but the ratio of the rates of religation of Top1–DNA cleavage complexes with either CPT or TFO remained almost the same irrespective of temperature (Table 1). Thus, the formation of a triplex 1 bp 3′ from the Top1-cleavage site enhances the steady-state Top1-mediated DNA cleavage by inhibiting religation. Moreover, presence of

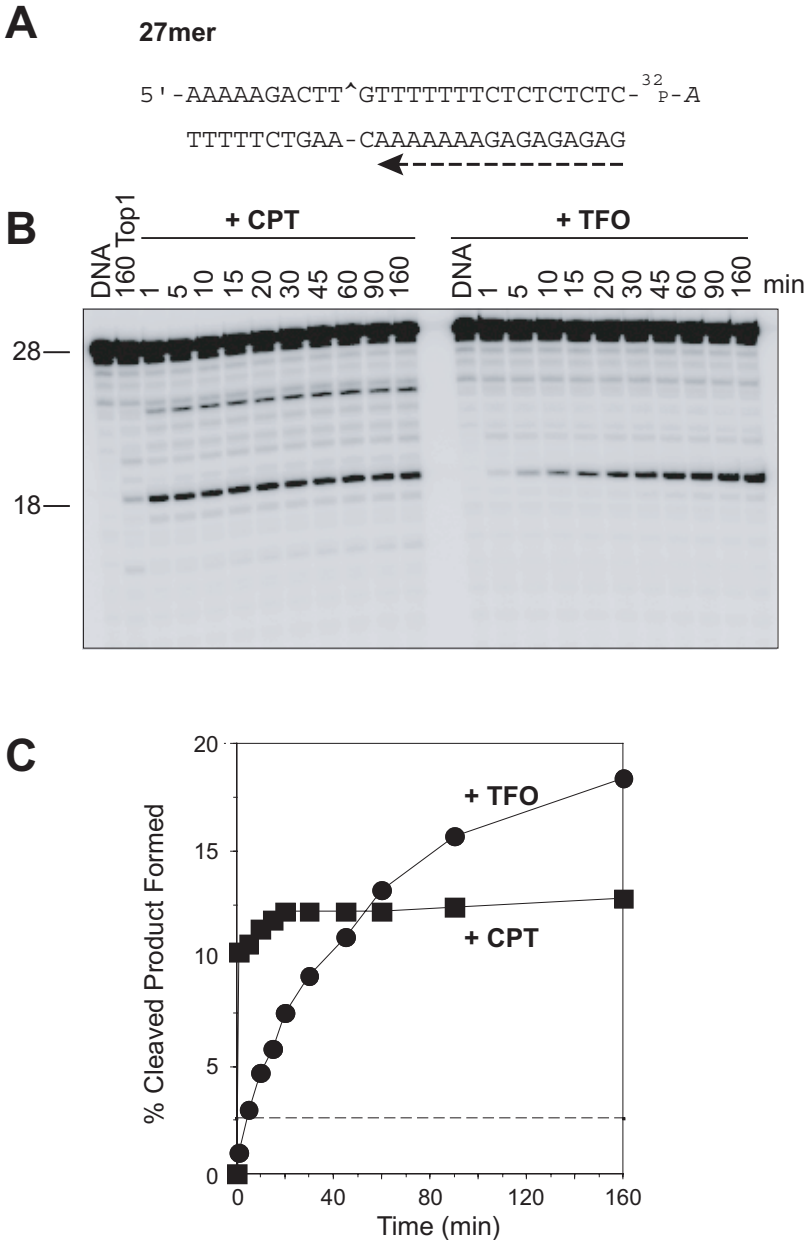

Figure 2. Triplex formation 1 bp 3′ from the Top1 site enhances steady-state DNA cleavage and slows down the forward rate of cleavage by Top1. (**A**) Sequence of the 27mer duplex DNA showing the orientation of the TFO by a dashed arrow. (**B**) The 27mer oligonucleotide was 3′ end labeled on the scissile strand and the corresponding triplex was formed (+TFO). The labeled 27mer oligonucleotide was reacted with Top1 in the absence of drug for 160 min (160 Top1) or in the presence of 1 μM CPT at 25°C for the indicated times (min). Similar reactions were carried out in the absence of CPT using the 27mer triplex oligonucleotide (+TFO) in the absence (DNA) or in the presence of Top1. Numbers 28 and 18 indicate the size of the 3′ labeled oligonucleotide and the Top1-mediated DNA fragment induced by TFO or CPT, respectively. (**C**) The Top1-mediated cleavage products obtained for CPT (square) and TFO (circle) were quantified and represented graphically. The horizontal dashed line corresponds to the Top1-mediated DNA cleavage in the absence of CPT or TFO. Computed kinetic constants are summarized in Table 1.

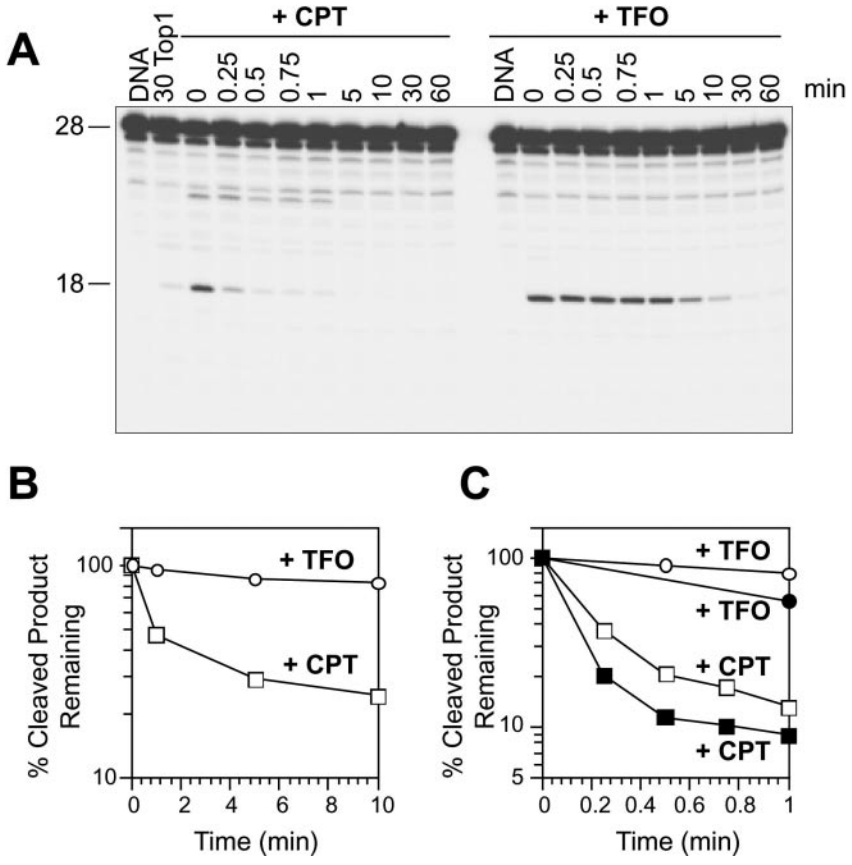

Figure 3. Triplex formation 1 bp 3′ from the Top1 cleavage site interferes with the Top1-mediated religation. (**A**) The 27mer oligonucleotide labeled on the 3′ end of the scissile strand (shown in Figure 1 and 2A) was reacted with Top1 in the absence of drug (+Top1) or in the presence of 1 μM CPT at 25°C for 30 min. The reactions were reversed in 0.35 M NaCl at 25°C for the indicated times (min). Time 0 refers to the samples taken immediately before the NaCl addition. Similar reactions were carried out using the 27mer triplex oligonucleotide (+TFO) in the absence (DNA) or in the presence of Top1 at 25°C for 30 min. The reactions were stopped before (0) and after reversal at 25°C for the indicated times (min). (**B** and **C**) Reactions as in (A) were carried out with salt reversals at 0°C (B), 25°C [(hollow squares and circles; (C)] or 37°C [filled squares and circles; (C)]. The percentage of the Top1-mediated cleavage products remaining after salt reversal for CPT (squares) and TFO (circles) were quantified and represented in semilog plots. Values are normalized to the drug-induced cleavage product remaining at time 0 taken as 100%. Computation of the reversal kinetic constants is summarized in Table 1.

Table 1. Cleavage and religation rate constants of CPT and TFO in the 27 and 30mer (I) oligonucleotides

	27mer						30mer (I)					
	0°C			25°C			25°C			0°C		
	CPT	TFO	Ratio TFO/CPT	CPT	TFO	Ratio TFO/CPT	CPT	TFO	Ratio TFO/CPT	CPT	TFO	Ratio TFO/CPT
$T_{1/2}$ (min)	4.5	76	16.88	0.15	3.9	26	0.36	<0.09	<0.25	7.6	<0.4	<0.05
k_2 (min^{-1})	0.15	0.009	0.06	4.62	0.18	0.04	1.93	>7.7	>4	0.087	>1.8	>20.69
k_1 (min^{-1})	NA	NA	NA	0.68	0.04	0.06	2.45	>2.99	>1.22	0.224	>1.41	>6.3
r	NA	NA	NA	0.13	0.19	1.46	0.56	0.28	0.5	0.72	0.44	0.61

$T_{1/2}$, Religation rate half-life determined from the salt reversal experiments (see Figures 3B, 3C, 4D, 4E, 5E and 6E); k_2, religation rate constant determined from $T_{1/2}$; k_1, cleavage rate constant (see Materials and Methods); r, the fraction of cleavage product at steady state (see Figures 2C, 4C, 5D and 6D); NA, not applicable as the Top1-mediated DNA cleavage failed to form measurably in the presence of TFO at 0°C.

this triplex also inhibits the nicking step, albeit to a lesser extent than the religation (closing) step (Table 1), thereby resulting in a net increase in steady-state cleavage (Figure 2C).

Formation of a triplex 4 bp 3′ from the Top1–DNA cleavage site enhances the rate of Top1-mediated cleavage

We next tested the relationship between Top1 activity and distance between the triplex–duplex junction and the Top1 site. In the 30mer (I), 4 bp were inserted between the triplex–duplex junction and the Top1 site (sequences shown in Figures 1 and 4A). Kinetics of the Top1-mediated DNA cleavage showed a rapid increase and saturation in the formation of the 21mer product with time both in the presence of TFO and CPT (Figure 4B and C).

Reversibility analyses of the Top1 cleavage complexes showed that the complexes induced by TFO in the 30mer (I) substrate (+TFO) reversed extremely fast, irrespective of

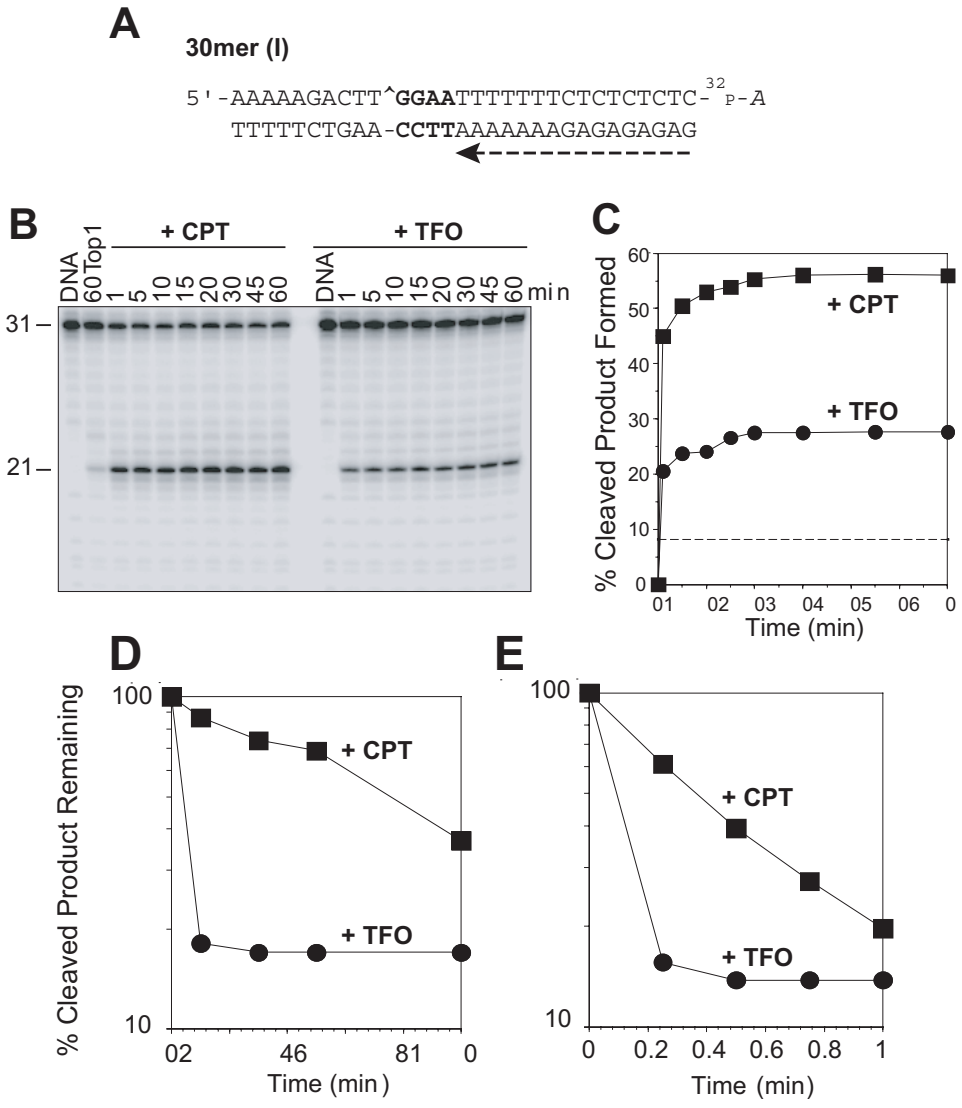

Figure 4. The Top1-mediated DNA cleavage complexes induced by TFO in the 30mer (I) oligonucleotide are rapidly reversible. (**A**) Sequence of the 30mer (I) duplex DNA showing the orientation of the TFO by a dashed arrow (see Figure 1). (**B**) Top1 cleavage reactions as in Figure 2B were carried out at 25°C using the 30mer (I) oligonucleotide (+CPT) and its corresponding triplex (+TFO) for the indicated times (min). Numbers 31 and 21 indicate the size of the 3′ labeled substrate oligonucleotide and the Top1-mediated DNA fragment, respectively. (**C**) Graphical representation of the data shown in panel B. The horizontal dashed line corresponds to the Top1-mediated DNA cleavage in the absence of TFO or CPT. (**D** and **E**) The Top1-mediated DNA cleavage products remaining after salt reversals at 0°C (Panel D) and 25°C (Panel E) for CPT (square) and TFO (circle) were quantified and represented graphically. Computed kinetic constants are summarized in Table 1.

the temperature of reversal (Figure 4D and E; Table 1) as compared with CPT (+CPT). Consequently, the rate of the cleavage reaction (k_1) was greater for TFO than for CPT (Table 1), although the amount of cleaved product was less for TFO than for CPT at equilibrium (Figure 4C and Table 1). A net increase in the 21mer cleavage product over time implies that the presence of the TFO 4 bp 3′ from the Top1 site enhances the forward cleavage (nicking) reaction.

Enhancement of the Top1-mediated DNA cleavage rate by triplexes 4 bp 3′ from the Top1 site is not affected by the intervening DNA sequence

By altering the DNA sequence between the site of Top1–DNA cleavage and the triplex–duplex junction from a –GGAA– (purine-rich) in the 30mer (I) to a –GCTA– in the 30mer (II) oligonucleotide (sequence shown in Figures 1 and 5A), we evaluated the contribution of the 4 bases purine-rich stretch, if any, to the enhancement of Top1 cleavage by the triplex seen in the 30mer (I) oligonucleotide. Kinetic analysis of the Top1-mediated DNA cleavage in the presence of triplex on the forward cleavage (Figure 5B and D) and on the reverse religation reaction (Figure 5C and E) in the 30mer (II) oligonucleotide showed no significant difference from that seen in the 30mer (I) oligonucleotide (see Figure 4). From Table 2, it can be deduced that the triplex formation in both 30mer (I) and 30mer (II) oligonucleotides shows faster rates for both cleavage (k_1) and religation (k_2) compared with CPT. Thus, the triplex formation starting 4 bp 3′ from the Top1–DNA cleavage site enhances the Top1 forward cleavage rate

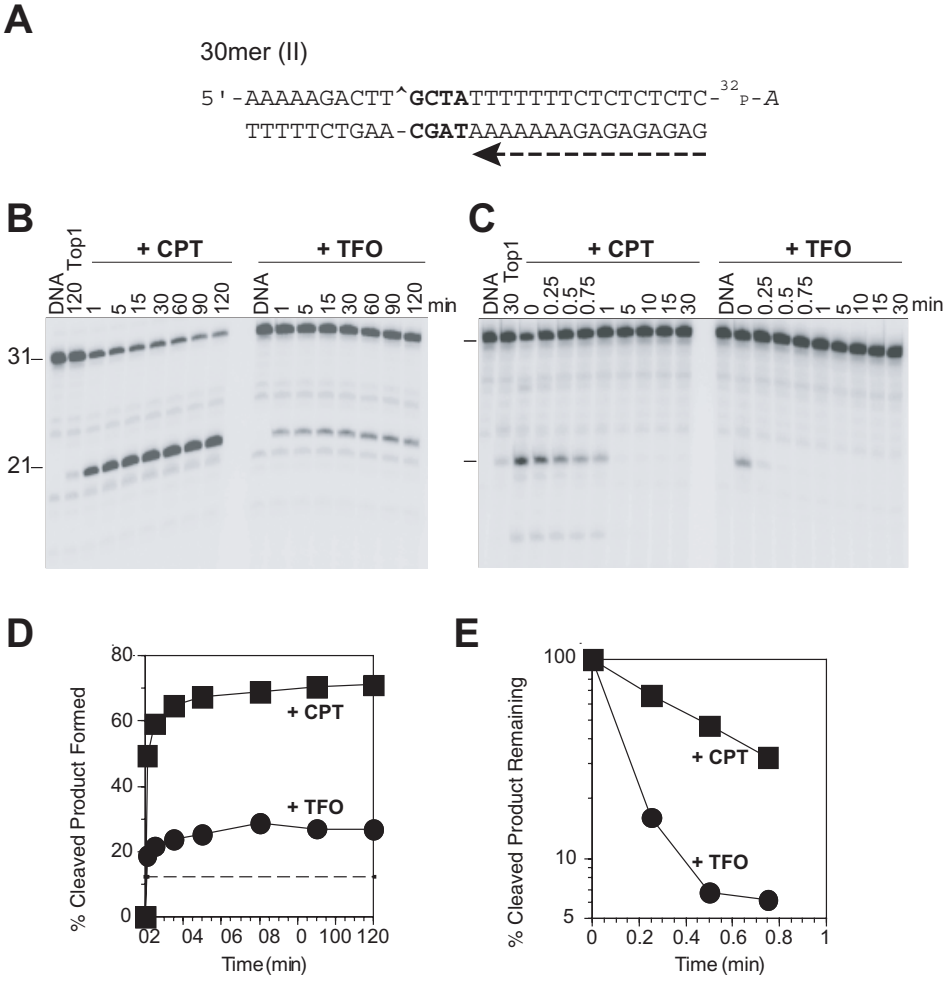

Figure 5. Altering the sequence between the Top1–DNA cleavage site and the duplex–triplex junction does not influence how the triplex formation affects Top1–DNA cleavage. (**A**) Sequence of the 30mer (II) duplex DNA showing the orientation of the TFO by a dashed arrow (see Figure 1). (**B**) Similar Top1 reactions as in Figures 2B and 4B were carried out using 3′ radiolabeled 30mer (II) oligonucleotide. (**C**) Using the same oligonucleotides as in panel B, salt reversal reactions (as in Figures 3 and 4D–E) were carried out at 25°C for the indicated times (min). Time 0 refers to the samples taken immediately before the NaCl addition. Numbers 31 and 21 indicate the size of the 3′ labeled oligonucleotide substrate and the Top1-mediated DNA fragment, respectively. (**D** and **E**) Graphical representation of the data in panels B and C, respectively. The horizontal dashed line in panel D corresponds to the Top1-mediated DNA cleavage in the absence of CPT or TFO. Computed kinetic constants are summarized in Table 2.

Table 2. Effect of local DNA sequences and the orientation of the TFO on the cleavage and religation rate constants of Top1–DNA cleavage complexes

	30mer (I)		30mer (II)		30mer (III)	
	CPT	TFO	CPT	TFO	CPT	TFO
$T_{1/2\ (min)}$	0.36	<0.09	0.45	<0.09	0.64	0.4
$k_{2\ (min^{-1})}$	1.93	>7.7	1.54	>7.7	1.1	1.7
$k_{1\ (min^{-1})}$	2.45	>2.99	3.8	>2.7	0.45	1.5
r	0.56	0.28	0.71	0.26	0.29	0.48

Reactions were performed at 25°C (see Table 1).

(k_1). Moreover, this enhancement is independent of the 4 bp duplex DNA sequence intervening between the Top1 cleavage site and the triplex junction.

Orientation of the triplex affects the Top1-mediated DNA religation

To evaluate the possible role of the orientation of the triplex with respect to the Top1-mediated DNA cleavage, we synthesized the 30mer (III) oligonucleotide (sequence shown in Figures 1 and 6A) containing the polypurine stretch on the scissile strand. The triplex is inserted in a reverse orientation compared to the 30mer (II) oligonucleotide with its 5′ end 4 bp 3′ from the Top1 cleavage site. Figure 6 shows that the triplex in the 30mer (III) oligonucleotide markedly enhanced Top1–DNA cleavage as compared with Top1 alone and even with Top1 + CPT. Though the amount of cleaved product formed was more with TFO (Figure 6B and D and Table 2; r value) than with CPT in the 30mer (III) oligonucleotide, the rate of the forward cleavage reaction (k_1) was slightly slower when compared to the 30mer (II) oligonucleotide (see Figure 5B and D and Table 2).

Kinetic analyses of the reversal rates (Figure 6C and E; Table 2) showed the religation rate (k_2) to be markedly slower in the presence of TFO in the 30mer (III) as compared to the 30mer (II) oligonucleotide (see Figure 5C and E; Table 2). Thus, the orientation of the triplex determines the step of the Top1-reaction affected. In the reverse orientation

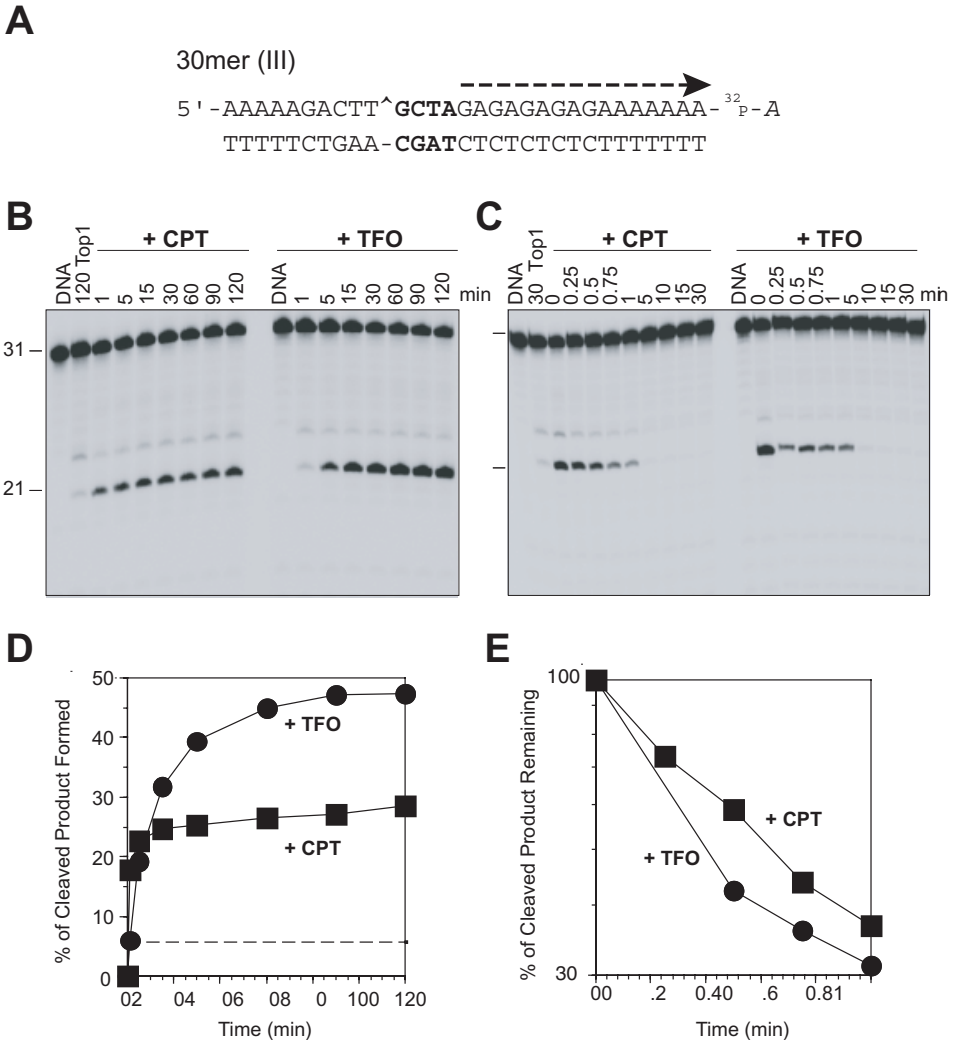

Figure 6. Inversion of the triplex orientation affects the reversal of the Top1-mediated DNA cleavage. (**A**) Sequence of the 30mer (III) duplex DNA showing the reverse orientation of the TFO compared with the 30mer (II) (see Figure 1). (**B**) Similar Top1 reactions as in Figures 2B, 4B and 5B were carried out using the 30mer (III) oligonucleotide. (**C**) Using the same oligonucleotides as in panel B, salt reversal reactions (as in Figures 3, 4D, 4E and 5C) were carried out at 25°C for the indicated times (min). Time 0 refers to the samples taken immediately before the NaCl addition. (**D** and **E**) Graphical representation of the data shown in panels B and C, respectively. The dashed line in panel D corresponds to the Top1-mediated DNA cleavage in the absence of CPT or TFO. Computed kinetic constants are summarized in Table 2.

[30mer (III)], the triplex formed 4 bp from the Top1 site enhances steady-state DNA cleavage primarily by inhibiting the Top1-mediated DNA religation.

Orientation and position of triplex formation affects the DNA twist at the Top1–DNA cleavage site differentially

By molecular calculations, we minimized the conformational energy (kcal) versus the twist (°) in the B-form DNA duplex, containing a nick at the Top1 cleavage site, in the absence (open circles) and presence (filled circles) of the triplex (Figure 7). In the 27mer target (Figure 7A), the torsion in the presence of the triple helix is displaced 2° downwards compared to the DNA alone, indicating that more energy is needed to religate the cleaved strand, in agreement with the results of the salt-reversal experiments. In both the 30mer (I) (data not shown) and 30mer (II) oligonucleotides (Figure 7B) modeling predicts that the two targets with TFOs are equivalent to the DNA alone. The width of the pit corresponding to the thermal energy at RT (0.5 kcal) is the same in these two targets, but it increases greatly in the case of 30mer (III) oligonucleotide (Figure 7C). The differential effect of triplex formation on the DNA twist in the four oligonucleotides could account for the differences in the affected Top1 reaction step: cleavage or religation. Graphic inspection and analysis of helical parameters of all the four models did not show pronounced structural distortion such as bending at the junction, except usual structural transition from triplex to duplex, which spans over 2–3 bp in duplex region. At this regard, the nick in 27mer target falls in such a triplex–duplex transition, and may explain the downward displaced twist profile because the triplex is underwound as compared to the duplex in B-form DNA.

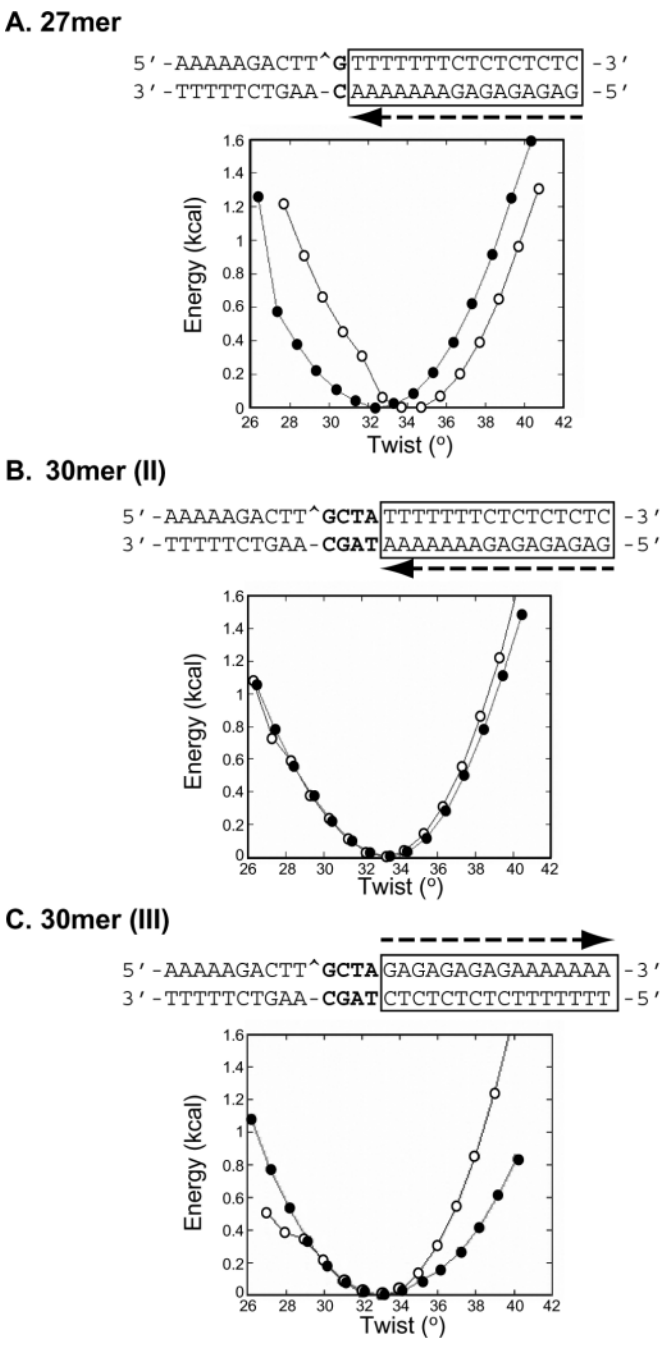

Figure 7. Effect of the triplex formation on the local flexibility at the scission site. By adiabatic mapping using conformational energy minimizations, the conformational energy (kcal) versus the twist (°) in the B-form DNA duplex, containing a nick at the Top1-cleavage site (shown by a caret in the sequence), in the absence (open circle) and in the presence of a triple helix (filled circle) in the 27mer (**A**), 30mer (II) (**B**) and 30mer III (**C**) oligonucleotides was determined and represented graphically. The sequences of the corresponding oligonucleotides are represented above the graphs showing the orientation of triplex formation by an arrow and the sequence it interacts within a box.

DISCUSSION

Top I has been extensively characterized in its ability to alter the topology of DNA and in its sensitivity to abnormal DNA structures (17,19–22,32–36). The crystal structure of Top1–DNA complexes has been resolved (18,37–39). Top1 can process four stranded structures, such as Holliday junctions (19,40), and binds to quadruplex DNA structures (41,42). The present study was carried out in an attempt to throw light on how triplexes affect Top1 activity.

For this purpose, we designed oligonucleotides bearing a strong Top1 cleavage site (19,23,43,44) flanked by a 16 bp oligopurine•oligopyrimidine triplex site to which a 16mer TFO containing 5-methyl-deoxycytosine (M) and 5-propynyl-2′-deoxyuridine (P) binds strongly and in well-characterized conditions (45). The Top1-mediated DNA cleavage site is situated either at the 3′ end of the triplex on the oligopyrimidine-containing strand of the duplex [oligonucleotides 27 and 30mer (I) and (II)] or at the 5′ end on the oligopurine-containing strand of the duplex [oligonucleotide 30mer (III)], respecting the geometry imposed by the formation of the cleavage complex (see Figure 1). Indeed, crystal structures show that Top1 encircles the DNA duplex with most of the enzyme contacts 5′ from the cleavage site. Therefore, the 5′ hydroxyl end of the broken DNA is free to rotate around the intact phosphodiester, which is essential for the Top1-mediated DNA relaxation (18,38,39,46).

To investigate how triplexes increase the steady-state level of DNA cleavage, we carried out kinetic analysis of the cleavage (nicking) and religation (closing) reactions. Religation experiments were carried out in the presence of salt to preserve the stability of triplex and duplex DNA structure (47). CPT was used as a 'positive control' since it is a known inhibitor of the Top1 religation reaction (9,30,31,48,49).

We find that several mechanisms are responsible for the enhancement of Top1-mediated DNA cleavage by TFO depending on the triplex position and orientation relative to the Top1 cleavage site. In the 27mer, because of the closeness of the triple-helical structure, the cleavage reaction is slow compared to CPT alone, but the reversal reaction is even slower (25 times) and the global effect is a higher steady-state cleavage (Figures 2 and 3; Table 1). Both the 30mer (I) and 30mer (II) substrates, bearing the cleavage site 4 bp 3′ from the 3′ triplex end, show a very different interference mechanism compared to the 27mer. Nevertheless, both 30mer (I) and (II) show similar behavior: increased cleavage. The fast reversal (Figures 4 and 5; Table 2) compared to CPT results in a less steady-state cleavage product. The similarity between the 30mer (I) and (II) substrates indicates no effect of changing the base pair sequence (from -G**GA**A- to -G**CT**A-) (see Figure 1) between the cleavage site and the duplex–triplex junction. However, upon reversing the triplex orientation, as in the 30mer (III) substrate, so that the cleavage site is on the 5′ side of the triplex on the oligopurine-containing strand of the duplex, DNA religation becomes inhibited like in the case of CPT and the 27mer triplex, and the steady-state cleavage is 2-fold higher than with CPT (Figure 6D and Table 2).

To elucidate the observed differences in the steps of the Top1 reaction that are affected by the different triplexes-containing oligonucleotides, we carried out modeling studies (see Figure 7). Based on molecular calculations (adiabatic mapping) after minimizing the conformational energy (kcal) versus the twist (°) in the B-form DNA duplex containing a nick at the Top1 cleavage site, we found that differences in the twist of DNA could account for the differences seen in the effect of the triplexes on the Top1-mediated DNA cleavage.

Figure 7A shows that in the 27mer target, the torsion in the presence of the triple helix is displaced 2° downwards compared to the DNA alone, indicating that more energy is needed to religate the cleaved strand. This is in agreement with the experimental data (Figure 3), showing, that in the presence of the triple helix, Top1 religates 25 times slower (Table 1), and, even if it cleaves more slowly, the net result is an increase in Top1 cleavage (Figure 2). The slower cleavage rate might be due to the proximity of the triplex junction, only one base from the Top1 cleavage site.

The two 30mer, 30mer (I) and (II), behave experimentally in a similar way: the rate of cleavage in the presence of the triple helix is faster than the one in CPT even if the fraction of cleavage product is decreased by half. On the other hand, the religation is at least four times faster than in the case of CPT (Tables 1 and 2). The modeling predicts that the two targets are equivalent to the DNA alone. The width of the pit corresponding to the thermal energy at RT (0.5 kcal) is also the same in these two targets (Figure 7B), but this was greatly increased in the case of 30mer (III) oligonucleotide (Figure 7C) where the orientation of the triplex is in reverse. Experimentally, the triplex in the 30mer (III) produced steady-state cleavage almost 2-fold higher compared to that with CPT (Figure 6D and Table 2). The interpretation is that in the first configuration [30mer (I) and (II)], the DNA twist at the cleavage site is similar to the DNA in the absence of TFO. This is consistent with normal religation. In the second case [30mer (III)], the local flexibility or dynamic twist is abnormal. The DNA is moving around at the site of cleavage, which might interfere with religation.

To our knowledge, the stimulation of the Top1 cleavage (nicking) step by the triplexes [as in 30 (I) and (II)] is rather unique. Until now, DNA modifications and Top1 inhibitors were found to block religation (19–21,44,50). Several scenarios can be envisaged to account for the stimulation of the DNA cleavage rate by triplexes. Major changes are observed in the conformation and/or dynamics of the minor groove in the presence of the triple helix (the minor groove is shallower and wider as compared to that in B-DNA). The size of the Crick–Hoogsteen groove varies with the sequence. DNase I cleavage is enhanced at the 3′ junction (51). When there are hydrophobic propynyl deoxyuridine in the third strand, the triplex has a bent appearance. It is established that the presence of a bent in DNA induced by a poly(dA)•poly(dT) tract on the region 3′ to the cleavage site stimulates Top1 binding and cleavage (52). Furthermore, experiments of the Top1-mediated relaxation of supercoiled DNA plasmid in the presence of triplex show DNA to be unwound (data not shown). Htun and Dahlberg (53) have shown that formation of an intramolecular triplex in supercoiled DNA results in relaxation of about one negative superhelical turn for every 11 bp of the repeat involved in triplex formation.

Our study shows that Top1 reactions can be differentially affected by multistranded structures like triplexes. Either by favoring the cleavage reaction or by inhibiting the religation reaction, triplexes enhance the Top1-mediated cleavage. The reaction affected depends on the relative position and orientation of the triplex with respect to the Top1 site. Localization of the TFO 1 bp from the cleavage site in the 3′ orientation or 4 bp from the cleavage site in the 5′ orientation inhibits the religation step, probably by distorting the 5′ end of the cleaved DNA so that it cannot be aligned for religation to the 3′ end linked to the tyrosyl moiety of Top1. Positioning the triplex 4 bp downstream from the Top1 cleavage site in the 3′ orientation favors the forward cleavage reaction. This probably could imply a distortion in the DNA structure that favors the Top1-mediated DNA cleavage. The significance of these effects, assuming that triplexes can form naturally or be used pharmacologically, remains to be further explored.

REFERENCES

1. Wang,J.C. (2002) Cellular roles of DNA topoisomerases: a molecular perspective. *Nature Rev. Mol. Cell. Biol.*, **3**, 430–440.
2. Champoux,J.J. (2001) DNA topoisomerases: structure, function, and mechanism. *Annu. Rev. Biochem.*, **70**, 369–413.
3. Pommier,Y., Pourquier,P., Fan,Y. and Strumberg,D. (1998) Mechanism of action of eukaryotic DNA topoisomerase I and drugs targeted to the enzyme. *Biochim. Biophys. Acta*, **1400**, 83–105.
4. Osheroff,N. (ed.) (1998) *DNA Topoisomerases*. Elsevier, Amsterdam.
5. Tian,L., Claeboe,C.D., Hecht,S.M. and Shuman,S. (2003) Guarding the genome: electrostatic repulsion of water by DNA suppresses a potent nuclease activity of topoisomerase IB. *Mol. Cell*, **12**, 199–208.
6. Pommier,Y. (1996) Eukaryotic DNA topoisomerase I: genome gatekeeper and its intruders, camptothecins. *Semin. Oncol.*, **23**, 1–10.
7. Chen,A.Y. and Liu,L.F. (1994) DNA topoisomerases: essential enzymes and lethal targets. *Annu. Rev. Pharmacol. Toxicol.*, **94**, 194–218.
8. Nitiss,J.L. and Wang,J.C. (1996) Mechanisms of cell killing by drugs that trap covalent complexes between DNA topoisomerases and DNA. *Mol. Pharmacol.*, **50**, 1095–1102.
9. Pommier,Y., Redon,C., Rao,A., Seiler,J.A., Sordet,O., Takemura,H., Antony,S., Meng,L.-H., Liao, Z.Y., Kehlhagen, G. *et al.* (2003) Repair of and checkpoint response to Topoisomerase I-modified DNA damage. *Mutat Res.*, **532**, 173–203.
10. Rich,A. (1993) DNA comes in many forms. *Gene*, **135**, 99–109.
11. Mills,M., Lacroix,L., Arimondo,P.B., Leroy,J.L., Francois,J.C., Klump,H. and Mergny,J.L. (2002) Unusual DNA conformations: implications for telomeres. *Curr. Med. Chem. Anti-Canc. Agents*, **2**, 627–644.
12. Hélène,C., Thuong,N.T. and Harel-Bellan,A. (1992) Control of gene expression by triple helix-forming oligonucleotides. The antigene strategy. *Ann. NY Acad. Sci.*, **660**, 27–36.
13. Hoyne,P.R., Gacy,A.M., McMurray,C.T. and Maher,L.J.,III (2000) Stabilities of intrastrand pyrimidine motif DNA and RNA triple helices. *Nucleic Acids Res.*, **28**, 770–775.
14. Goni,J.R., de la Cruz,X. and Orozco,M. (2004) Triplex-forming oligonucleotide target sequences in the human genome. *Nucleic Acids Res.*, **32**, 354–360.
15. Giovannangeli,C. and Hélène,C. (2000) Triplex-forming molecules for modulation of DNA information processing. *Curr. Opin. Mol. Ther.*, **2**, 288–296.
16. Arimondo,P.B., Boutorine,A., Baldeyrou,B., Bailly,C., Kuwahara,M., Hecht,S.M., Sun,J.-S., Garestier,T. and Hélène,C. (2002) Design and optimization of camptothecin conjugates of triple helix-forming oligonucleotides for sequence-specific DNA cleavage by topoisomerase I. *J. Biol. Chem.*, **277**, 3132–3140.
17. Arimondo,P.B., Angenault,S., Halby,L., Boutorine,A., Schmidt,F., Monneret,C., Garestier,T., Sun,J.S., Bailly,C. and Hélène,C. (2003) Spatial organization of topoisomerase I-mediated DNA cleavage induced by camptothecin-oligonucleotide conjugates. *Nucleic Acids Res.*, **31**, 4031–4040.
18. Redinbo,M.R., Stewart,L., Kuhn,P., Champoux,J.J. and Hol,W.G.J. (1998) Crystal structure of human topoisomerase I in covalent and noncovalent complexes with DNA. *Science*, **279**, 1504–1513.
19. Pourquier,P., Ueng,L.-M., Kohlhagen,G., Mazumder,A., Gupta,M., Kohn,K.W. and Pommier,Y. (1997) Effects of uracil incorporation, DNA mismatches, and abasic sites on cleavage and religation activities of mammalian topoisomerase I. *J. Biol. Chem.*, **272**, 7792–7796.
20. Pourquier,P., Ueng,L.-M., Fertala,J., Wang,D., Park,H.-J., Essigman,J.M., Bjornsti,M.-A. and Pommier,Y. (1999) Induction of reversible complexes between eukaryotic DNA topoisomerase

I and DNA-containing oxidative base damages. *J. Biol. Chem.*, **274**, 8516–8523.
21. Pommier,Y., Laco,G.S., Kohlhagen,G., Sayer,J.M., Kroth,H. and Jerina,D.M. (2000) Position-specific trapping of topoisomerase I-DNA cleavage complexes by intercalated benzo[a]- pyrene diol epoxide adducts at the 6-amino group of adenine. *Proc. Natl Acad. Sci. USA*, **97**, 10739–10744.
22. Lesher,D.T., Pommier,Y., Stewart,L. and Redinbo,M.R. (2002) 8-Oxoguanine rearranges the active site of human topoisomerase I. *Proc. Natl Acad. Sci. USA*, **99**, 12102–12107.
23. Andersen,A.H., Gocke,E., Bonven,B.J., Nielsen,O.F. and Westergaard,O. (1985) Topoisomerase I has a strong binding preference for a conserved hexadecameric sequence in the promoter region of the rRNA gene from *Tetrahymena pyriformis*. *Nucleic Acids Res.*, **13**, 1543–1557.
24. Cantor,C.R., Warshaw,M.M. and Shapiro,H. (1970) Oligonucleotide interactions. 3. Circular dichroism studies of the conformation of deoxyoligonucleotides. *Biopolymers*, **9**, 1059–1077.
25. Antony,S., Jayaraman,M., Laco,G., Kohlhagen,G., Kohn,K.W., Cushman,M. and Pommier,Y. (2003) Differential induction of topoisomerase I-DNA cleavage complexes by the indenoisoquinoline MJ-III-65 (NSC 706744) and camptothecin: base sequence analysis and activity against camptothecin-resistant topoisomerases I. *Cancer Res.*, **63**, 7428–7435.
26. Lavery,R. and Sklenar,H. (1988) The definition of generalized helicoidal parameters and of axis curvature for irregular nucleic acids. *J. Biomol. Struct. Dyn.*, **6**, 63–91.
27. Lavery,R., Sklenar,H., Zakrzewska,K. and Pullman,B. (1986) The flexibility of the nucleic acids: (II). the calculation of internal energy and applications to mononucleotide repeat DNA. *J. Biomol. Struct. Dyn.*, **3**, 989–1014.
28. Chomilier,J., Sun,J.S., Collier,D.A., Garestier,T., Hélène,C. and Lavery,R. (1992) A computational and experimental study of the bending induced at a double-triple helix junction. *Biophys. Chem.*, **45**, 143–152.
29. Ouali,M., Letellier,R., Adnet,F., Liquier,J., Sun,J.S., Lavery,R. and Taillandier,E. (1993) A possible family of B-like triple helix structures: comparison with the Arnott A-like triple helix. *Biochemistry*, **32**, 2098–2103.
30. Hsiang,Y.H., Hertzberg,R., Hecht,S. and Liu,L.F. (1985) Camptothecin induces protein-linked DNA breaks via mammalian DNA topoisomerase I. *J. Biol. Chem.*, **260**, 14873–14878.
31. Tanizawa,A., Kohn,K.W., Kohlhagen,G., Leteurtre,F. and Pommier,Y. (1995) Differential stabilization of eukaryotic DNA topoisomerase I cleavable complexes by camptothecin derivatives. *Biochemistry*, **34**, 7200–7206.
32. Pourquier,P. and Pommier,Y. (2001) Topoisomerase I-mediated DNA damage. *Adv. Cancer Res.*, **80**, 189–216.
33. Wang,X., Henningfeld,K.A. and Hecht,S.M. (1998) DNA topoisomerase I-mediated formation of structurally modified DNA duplexes. Effects of metal ions and topoisomerase I inhibitors. *Biochemistry*, **37**, 2691–2700.
34. Cheng,C. and Shuman,S. (2000) Recombinogenic flap ligation pathway for intrinsic repair of topoisomerase IB-induced double-strand breaks. *Mol. Cell. Biol.*, **20**, 8059–8068.
35. Sekiguchi,J., Cheng,C. and Shuman,S. (1997) Kinetic analysis of DNA and RNA strand transfer reactions catalyzed by vaccinia topoisomerase. *J. Biol. Chem.*, **272**, 15721–15728.
36. Yakovleva,L., Tian,L., Sayer,J.M., Kalena,G.P., Kroth,H., Jerina,D.M. and Shuman,S. (2003) Site-specific DNA transesterification by vaccinia topoisomerase: effects of benzo[alpha]pyrene-dA, 8-oxoguanine, 8-oxoadenine and 2-aminopurine modifications. *J. Biol. Chem.*, **278**, 42170–42177.
37. Redinbo,M.R., Champoux,J.J. and Hol,W.G. (2000) Novel insights into catalytic mechanism from a crystal structure of human topoisomerase I in complex with DNA. *Biochemistry*, **39**, 6832–6840.
38. Stewart,L., Redinbo,M.R., Qiu,X., Hol,W.G. and Champoux,J.J. (1998) A model for the mechanism of human topoisomerase I. *Science*, **279**, 1534–1541.
39. Redinbo,M.R., Stewart,L., Champoux,J.J. and Hol,W.G. (1999) Structural flexibility in human topoisomerase I revealed in multiple non-isomorphous crystal structures. *J. Mol. Biol.*, **292**, 685–696.
40. Liao,S., Mao,C., Birktoft,J.J., Shuman,S. and Seeman,N.C. (2004) Resolution of undistorted symmetric immobile DNA junctions by vaccinia topoisomerase I. *Biochemistry*, **43**, 1520–1531.
41. Arimondo,P.B., Riou,J.F., Mergny,J.L., Tazi,J., Sun,J.S., Garestier,T. and Hélène,C. (2000) Interaction of human DNA topoisomerase I with G-quartet structures. *Nucleic Acids Res.*, **28**, 4832–4838.
42. Marchand,C., Pourquier,P., Laco,G.S., Jing,N. and Pommier,Y. (2002) Interaction of human nuclear topoisomerase I with guanosine quartet-forming and guanosine-rich single-stranded DNA and RNA oligonucleotides. *J. Biol. Chem.*, **277**, 8906–8911.
43. Bonven,B.J., Gocke,E. and Westergaard,O. (1985) A high affinity topoisomerase I binding sequence is clustered at DNAase I hypersensitive sites in Tetrahymena R-chromatin. *Cell*, **41**, 541–551.
44. Pourquier,P., Pilon,A.A., Kohlhagen,G., Mazumder,A., Sharma,A. and Pommier,Y. (1997) Trapping of mammalian topoisomerase I and recombinations induced by damaged DNA containing nicks or gaps. Importance of DNA end phosphorylation and camptothecin effects. *J. Biol. Chem.*, **272**, 26441–26447.
45. Arimondo,P.B., Bailly,C., Boutorine,A.S., Moreau,P., Prudhomme,M., Sun,J.S., Garestier,T. and Hélène,C. (2001) Triple helix-forming oligonucleotides conjugated to indolocarbazole poisons direct topoisomerase I-mediated DNA cleavage to a specific site. *Bioconjug. Chem.*, **12**, 501–509.
46. Laco,G.S., Collins,J.R., Luke,B.T., Kroth,H., Sayer,J.M., Jerina,D.M. and Pommier,Y. (2002) Human topoisomerase I inhibition: docking camptothecin and derivatives into a structure-based active site model. *Biochemistry*, **41**, 1428–1435.
47. Plum,G.E. and Breslauer,K.J. (1995) Thermodynamics of an intramolecular DNA triple helix: a calorimetric and spectroscopic study of the pH and salt dependence of thermally induced structural transitions. *J. Mol. Biol.*, **248**, 679–695.
48. Kjeldsen,E., Svejstrup,J.Q., Gromova,I.I., Alsner,J. and Westergaard,O. (1992) Camptothecin inhibits both the cleavage and religation reactions of eukaryotic DNA topoisomerase I. *J. Mol. Biol.*, **228**, 1025–1030.
49. Jaxel,C., Kohn,K.W. and Pommier,Y. (1988) Topoisomerase I interaction with SV40 DNA in the presence and absence of camptothecin. *Nucleic Acids Res.*, **16**, 11157–11170.
50. Pommier,Y., Kohlhagen,G., Pourquier,P., Sayer,J.M., Kroth,H. and Jerina,D.M. (2000) Benzo[a]pyrene diol epoxide adducts in DNA are potent suppressors of a normal topoisomerase I cleavage site and powerful inducers of other topoisomerase I cleavages. *Proc. Natl Acad. Sci. USA*, **97**, 2040–2045.
51. Cassidy,S.A., Strekowski,L., Wilson,W.D. and Fox,K.R. (1994) Effect of a triplex-binding ligand on parallel and antiparallel DNA triple helices using short unmodified and acridine-linked oligonucleotides. *Biochemistry*, **33**, 15338–15347.
52. Krogh,S., Mortensen,U.H., Westergaard,O. and Bonven,B.J. (1991) Eukaryotic topoisomerase I-DNA interaction is stabilized by helix curvature. *Nucleic Acids Res.*, **19**, 1235–1241.
53. Htun,H. and Dahlberg,J.E. (1989) Topology and formation of triple-stranded H-DNA. *Science*, **243**, 1571–1576.